INL/EXT-20-59992

NRC Multiphysics Analysis Capability Deployment FY 2020 - Part 4

Javier Ortensi[1], Matthew P. Johnson [2], Zachary M. Prince[3], Mark D. DeHart[1]

[1] Reactor Physics Design and Analysis
[2] ATR Reactor Nuclear Safety
[3] Nuclear Engineering Methods Development

Idaho National Laboratory
P.O. Box 1625
Idaho Falls, ID 83415-1347

September 2020

INL is a U.S. Department of Energy National Laboratory operated by Battelle Energy Alliance

INL/EXT-20-59992

NRC Multiphysics Analysis Capability Deployment FY 2020 - Part 4

Javier Ortensi, Matthew P. Johnson, Zachary M. Prince, Mark D. DeHart

September 2020

Idaho National Laboratory
Nuclear Science & Technology Division
Idaho Falls, Idaho 83415

http://www.inl.gov

Prepared for the
Office of Nuclear Regulatory Research
U. S. Nuclear Regulatory Commission
Washington, D. C. 20555
Task Order No.: 31310019F0015

Abstract

This report details progress and activities of Idaho National Laboratory (INL) on the Nuclear Regulatory Commission (NRC) project "Development and Modeling Support for Advanced Non-Light Water Reactors."

The tasks completed for this report are:

- Task 3a: This task demonstrates the effectiveness of Griffin's methods for interpolating cross sections and SPH correction factors as a function of control drum rotation. The Monte Carlo code Serpent is used to generate reference results. The accuracy of Griffin-calculated eigenvalues and reaction rates are studied as a function of control drum rotation for cross section and SPH factor libraries of varying fidelity. Higher-fidelity libraries require less interpolation and are therefore inherently more accurate; however, they require more computational resources to create. Overall, Griffin is able to accurately model eigenvalue and reaction rates over the full range of drum rotation using a library generated from three to five discrete drum rotations for a particular microreactor design.
- Task 3c: This preliminary task successfully demonstrates the performance of a coupled neutron-photon transport calculation with Griffin using the spherical harmonics approximation. The Griffin solutions are compared to reference solutions from the continuous energy Monte Carlo codes MCNP and Serpent. Furthermore, this work also demonstrates how to prepare the neutron and photon libraries using NJOY, MCNP, and Serpent with the latest ENDF/B-VIII data for ^{235}U and graphite. The Griffin total energy deposition in the active core region is calculated within 0.3% of the reference, but it degrades in the reflector regions with a maximum difference of -1.5%. Overall, the results look promising and future analysis should use an improved data stream and focus on determining the potential cancellation of error within each energy group.

Contents

List of Figures

List of Tables

1 INTRODUCTION

This report details progress and activities of Idaho National Laboratory (INL) on the Nuclear Regulatory Commission (NRC) project "Development and Modeling Support for Advanced Non-Light Water Reactors."

Table 1 provides a summary of the tasks completed for this report. It matches the deliverable number, the Statement-of-Work (SOW) number, and a short description of the deliverable to the relevant section in this report.

Table 1: List of deliverables

Deliverable Number	SOW Task	Report Section	Description
3a	3a*	2	improved control rod treatment
3c	3c*	3	heat generation in graphite moderator

* Task 3a and 3c were delayed until 9/2020.

The tasks completed for this report are:

- Task 3a: Improve control rod treatment. Develop heterogeneous control-rod model and test cusping treatment. In particular, ensure that diffusion with SPH can be used for control rod withdrawal events.
- Task 3c: Develop the capability to calculate the heat-generation rate in the graphite moderator and reflector regions due to gamma and neutron interactions.

2 VERIFICATION OF CONTROL DRUM MODELING WITH THE SPH METHOD

The Precondioned Jacobian-Fee Newton-Krylov SuperHomogenization (PJFNK-SPH) methodology in Griffin [1] allows the exact recovery of the reference group-wise reaction rates in each SuperHomogenization (SPH) region for a 3-D reactor core. For example, if the movement of a control rod is tabulated at various control rod positions, the PJFK-SPH method would preserve the eigenvalue and reaction rates in the SPH corrected regions at the discrete tabulation points. A challenge with this approach arises when the control rod is positioned in between the tabulation points. In this case, Griffin performs a linear interpolation of the SPH factors to approximate the reaction rates. In addition, the modeling of control rods and drum in deterministic methods is often complicated by the phenomena know as the *cusping effect*. Griffin includes a cusping treatment [2] that ameliorates the impact of this effect.

The purpose of this task is to ascertain if the methods in Griffin are adequate to model the movement of control drums. This analysis studies the combined SPH and the cusping treatments in Griffin in the case where the control drum itself is not included in the SPH correction.

2.1 Model Description

The microreactor model similar to that developed in [3] is employed here to verify Griffin's treatment of control drum rotation. Selected reactor characteristics are given in Table 2.

Table 2: Microreactor characteristics

thermal power	5 MW
fuel material	U-10Zr, 18.1% enriched
# of fuel elements	192
fuel lattice	hexagonal
lattice pitch	5.4 cm
reflector material	Al_20_3
control drum poison	B_4C

2.2 Results

A 2-D model is used to investigate how well SPH factor interpolation captures control-drum rotation. A 2-D model is sufficient to capture cusping effects since the control drums rotate in the xy plane around the z axis. In this exercise, a single control drum is rotated from fully in (poison nearest core center) (0°) to fully out (poison outward facing) (180°). Figures 1, 2, and 3 show the control drum at 0°, 90°, and 180°.

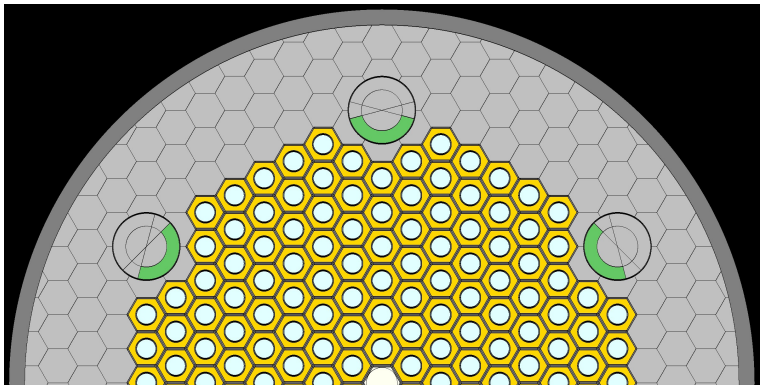

Figure 1: Serpent model with all drums at 0° rotation

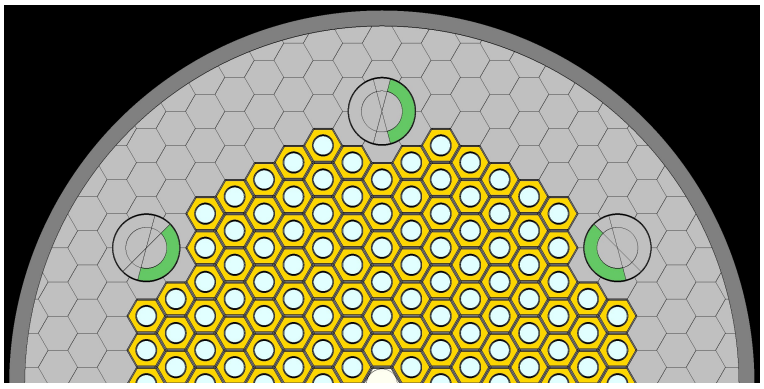

Figure 2: Serpent model with north drum at 90° rotation

Two Serpent models are used in this analysis. The first is a conventionally built model. The second takes the first model and sub-divides it into separate universes that match the discretization of the deterministic Griffin model. The second model is used to generate multigroup cross sections and reference fluxes for the SPH factor calculation. The sub-dividing is not something the analyst has to do by hand. The software stack being developed

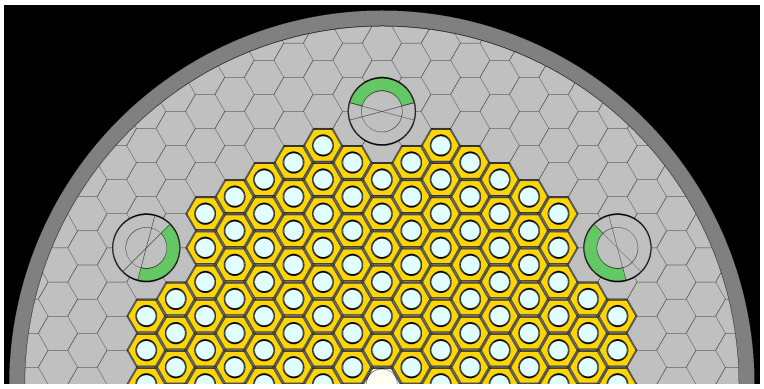

Figure 3: Serpent model with north drum at 180° rotation

with Griffin includes scripts that generate the mesh for the deterministic calculation and the appropriate Serpent model modifications. Since the subdividing adds additional complexity to the model, it is necessary to verify that both models are equivalent. Table 3 compares the core eigenvalue as a function of drum rotation for both Serpent models. The two models are equivalent within Monte Carlo uncertainty.

In order to study the effectiveness of SPH factor interpolation, a limited number of control drum rotation points are used to build cross section and SPH factor libraries for the deterministic model. The deterministic model uses SPH correction in the fuel elements and the first ring of the reflector. Table 4 shows the four cases that are studied. The first case is used as a limiting worst-case to show the effect of interpolation with too few points. Referring back to Figures 1, 2, and 3, it can be seen that the 0° and 180° grid points contain no information on what direction the drum rotates. The fourth case is the reference case that produces cross sections and reference fluxes for every rotation point studied in this analysis so no interpolation is needed.

Figure 4 shows the error in k_{eff} for the three interpolation cases. All cases reproduce the eigenvalue at their SPH grid points. Cases 1 and 2 underestimate drum worth in the first half of the rotation and overestimate worth in the second half. This same trend is seen to a lesser extent in Case 3.

The accuracy of interpolating reaction rates in SPH-corrected regions of the model is also studied. Figures 5 and 6 show the max error and root mean square error in the $\nu\Sigma_f$ reaction rate in all fuel regions and all energy groups. The limiting case, Case 1, is significantly less accurate than cases 2 and 3

Table 3: Serpent model comparison

	Serpent model	
rotation	reference	homogenization
0°	1.07308 ± 0.000034	1.07304 ± 0.000034
10°	1.07311 ± 0.000034	1.07310 ± 0.000034
20°	1.07323 ± 0.000032	1.07323 ± 0.000032
30°	1.07348 ± 0.000034	1.07353 ± 0.000032
40°	1.07383 ± 0.000032	1.07382 ± 0.000032
50°	1.07426 ± 0.000032	1.07428 ± 0.000032
60°	1.07472 ± 0.000032	1.07472 ± 0.000034
70°	1.07527 ± 0.000032	1.07523 ± 0.000032
80°	1.07582 ± 0.000032	1.07584 ± 0.000032
90°	1.07640 ± 0.000034	1.07640 ± 0.000032
100°	1.07697 ± 0.000032	1.07698 ± 0.000034
110°	1.07754 ± 0.000032	1.07753 ± 0.000032
120°	1.07803 ± 0.000032	1.07808 ± 0.000034
130°	1.07851 ± 0.000032	1.07854 ± 0.000035
140°	1.07893 ± 0.000032	1.07894 ± 0.000035
150°	1.07925 ± 0.000032	1.07925 ± 0.000032
160°	1.07953 ± 0.000032	1.07950 ± 0.000032
170°	1.07966 ± 0.000032	1.07967 ± 0.000032
180°	1.07970 ± 0.000032	1.07972 ± 0.000032

Table 4: SPH grid points

case	SPH grid points
case 1	0°, 180°
case 2	0°, 90°, 180°
case 3	0°, 40°, 90°, 140°, 180°
case 4	0° – 180°, every 10°

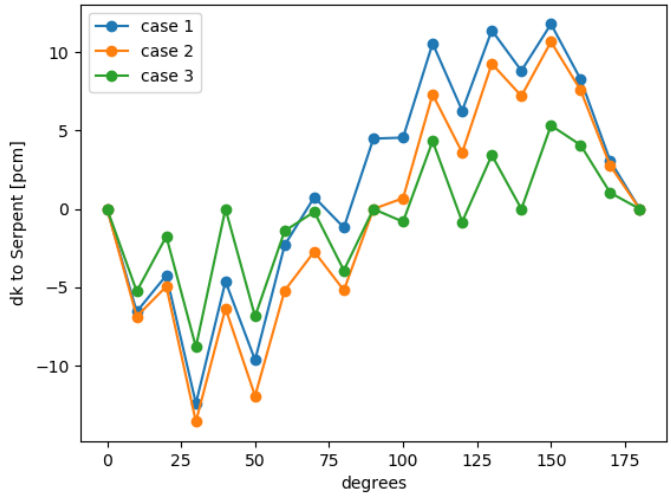

Figure 4: Error in k_{eff}

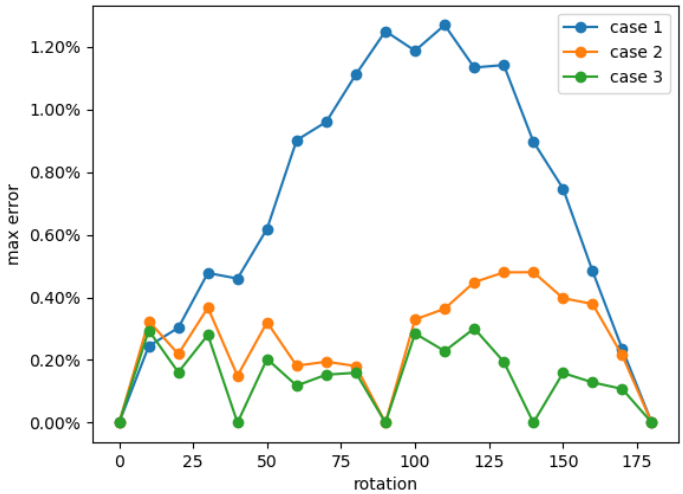

Figure 5: Max error in $\nu\Sigma_f\phi$

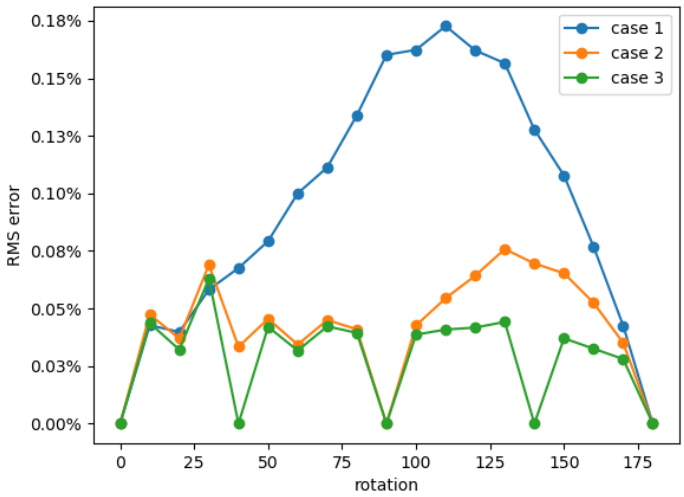

Figure 6: RMS error in $\nu\Sigma_f\phi$

Figures 7 and 8 show the error in integrated fuel element power at the control drum rotation which had the largest error in $\nu\Sigma_f\phi$. The reference fuel element powers are taken from Case 4.

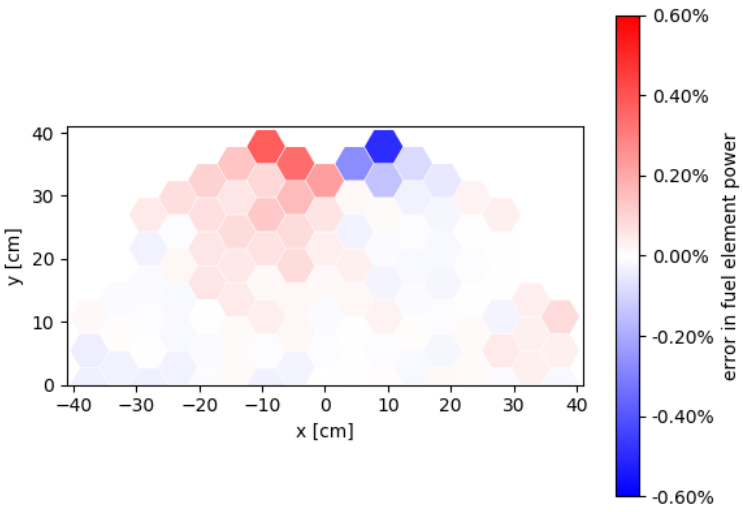

Figure 7: Error fuel element power, Case 2 at 140°

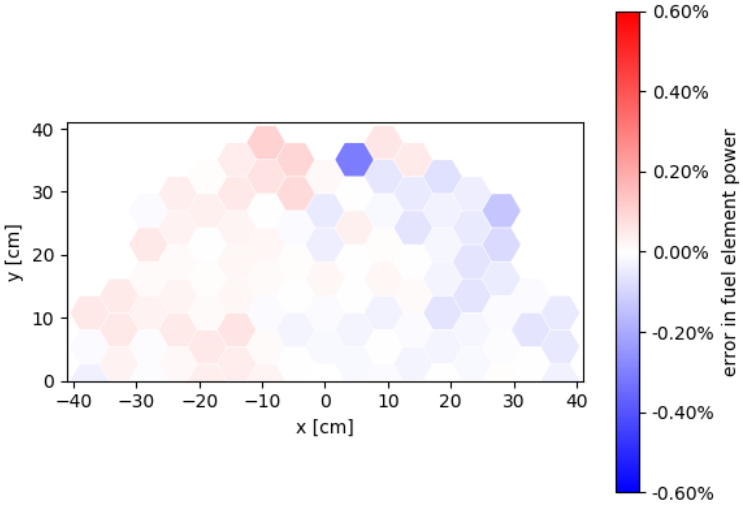

Figure 8: Error fuel element power, Case 3 at 120°

3 NON-LOCAL HEAT DEPOSITION IN GRAPHITE MODERATED REACTORS

The energy deposition from photon and neutron interactions in certain nuclear reactor structures can be important. This is particularly true in graphite reactors, where the heating of the control rods and reflectors can have a significant impact on their temperature and performance during accident scenarios. The purpose of this section is to demonstrate Griffin's capabilities to perform coupled neutron-photon heating calculations. The various codes used in this work are introduced in Section 3.1. The preparation of data is fundamental in the performance of neutron-photon heating calculations and is discussed in Section 3.2. A description of a simplified model of a graphite reactor with an active core containing dispersed ^{235}U in graphite and a graphite reflector in included in Section 3.3. Finally, the results form the various simulations are shown and discussed in Section 3.4.

3.1 Computer Codes

MCNP 6.1 [4] is a three-dimensional (3-D) continuous and multigroup energy Monte Carlo code developed at Los Alamos National Laboratory. MCNP has the capability to perform coupled neutron-photon transport calculations.

Serpent 2.1.32 beta [5] is a 3-D continuous-energy Monte Carlo reactor physics code developed at VTT Technical Research Centre of Finland. Serpent was selected because it offers 3-D spatial homogenization and group constant generation for deterministic reactor simulator calculations.

NJOY21 nuclear data processing system [6] is a modular computer code used for converting Evaluated Nuclear Data File (ENDF) format into libraries useful for applications calculations.

The Griffin code is a deterministic reactor physics and particle transport application under development jointly between Argonne National Laboratory and Idaho National Laboratory.

All computer codes used in this study employ the latest ENDF/B-VIII.r0 neutron data release. A special version of Serpent was obtained from the developer that supports ENDF/B-VIII data and the continuous S(a,b) formalism.

3.2 Data Preparation

The latest Griffin version has the capability to prepare fast reactor neutron and photon interaction cross-section data, but currently it cannot prepare these data sets for thermal reactors (i.e., graphite moderated reactors). The Serpent code can prepare the majority of the neutron interaction cross sections with the exception of the gamma production matrix. This matrix associates the neutron reaction cross section for photon-producing interactions to the number of photons generated in each photon energy group. Therefore, it is an GxM matrix, where G is the number of neutron energy groups and M is the number of photon energy groups. The NJOY code is used to prepare the gamma production matrix and the task entails the following calculation sequence:

1. Reconstruction of point-wise neutron energy-dependent data with module RECONR
2. Doppler broadening of the neutron cross sections with module BROADR
3. Computation of effective self-shielded neutron cross sections in the unresolved resonance range with module UNRESR, if the isotope contains resonance data
4. Computation of point-wise heat production neutron and photon cross sections with module HEATR
5. Generation of group-to-group neutron transfer matrices in the thermal range with module THERMR
6. Preparation of the neutron energy group dependent cross section and gamma production matrix with an approximated energy spectrum in module GROUPR
7. Production of a MATXS formatted file with the MATXSR module.

The weighting function (neutron spectrum) used in NJOY is approximated with a 172 neutron-energy group spectrum from the core region of the full core Monte Carlo calculation. This is far from ideal since one desires the most accurate representation of the neutron spectrum to perform the neutron energy condensation step. The capability to use better resolution is under development in Griffin and should be available in FY-21. The results from the NJOY data preparation show that the total photon production for each neutron energy group is not consistent between the NJOY and the MCNP reference, as shown in Figure 9. Therefore, the photon production matrix is rescaled to preserve the MCNP total photon production in each neutron energy group. In essence, this modifies only the magnitude of

the values, but preserves the shape. This is a necessary approximation until the gamma production matrix capability is added to Griffin. The scaling factor is computed with

$$S_{\gamma,m} = \frac{\Sigma_{\gamma,g}^{ref}}{\sum_{g=1}^{G} A_{g,m}}, \tag{1}$$

where

- $\Sigma_{\gamma,g}^{ref}$ is the reference total photon production cross section for neutron group g
- A_{GxM} is the photon production matrix from NJOY
- m is the column index in A_{GxM} (i.e., the photon energy group index)
- $S_{\gamma,m}$ is the scaling factor for column m.

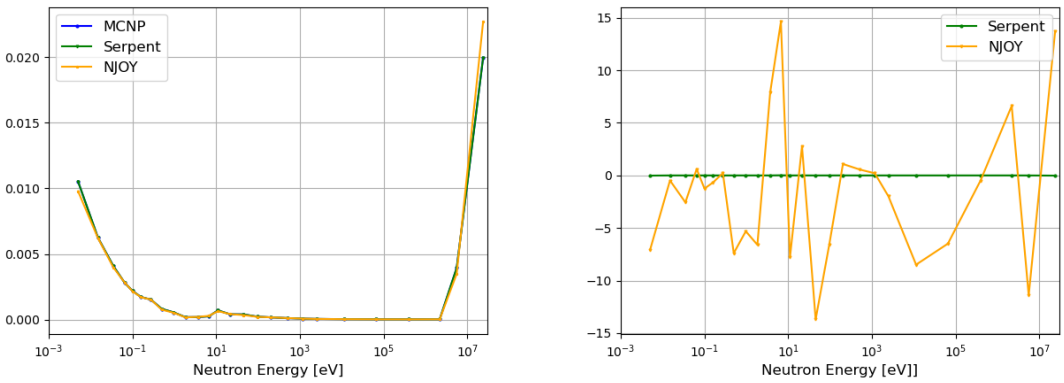

(a) Cross section [cm^{-1}]

(b) % Difference in cross section

Figure 9: Comparison of the total photon production cross section

The Serpent neutron cross sections are generated in the Griffin ISOXML format with the Griffin ISOXML module. The MATXS formatted file is processed with the Python script *read_matxs.py* to generate the photon production matrix. This Python script calculates the final photon production matrices for each isotope by adding the photon production matrices from various contributions: fission, elastic scattering, 39 inelastic scattering states, 35

alpha, n-gamma, n-2n, n-3n, n-Xn balance, neutron in the continuum (above discrete representation), and proton in the continuum. This is followed by the mixing of the isotopes. The script uses functions to rescale the matrices from inputted MCNP photon production values in each neutron energy group. Finally, the Python script appends the ISOXML file with the final macroscopic gamma production matrix and macroscopic neutron energy deposition cross sections.

Neither MCNP nor Serpent can generate all of the necessary photon transport cross sections needed for Griffin. MCNP is better suited to prepare some of the data, since several tallies can generate the group dependent total, photoelectric absorption, coherent (Raleigh), incoherent (Compton), and pair production reaction rates, which can then be divided by the flux to obtain the cross section:

$$\sigma_{x,m} = \frac{\int_{E_m}^{E_{m-1}} \int_\Omega \int_V \sigma_x(E,\Omega,r)\psi(E,\Omega,r)dEd\Omega dr}{\int_{E_m}^{E_{m-1}} \int_\Omega \int_V \psi(E,\Omega,r)dEd\Omega dr}, \tag{2}$$

where

- E, Ω, r are the energy, angular, and spatial variables, respectively
- $\sigma_{x,m}$ is the cross section for reaction x in photon energy group m
- ψ is the energy-dependent angular flux
- group m is defined between the upper and lower energy limits (E_{m-1}, E_m).

The group-to-group transfer matrices are not available in MCNP, but can be obtained with the GAMINR module in NJOY. The weighting function (photon spectrum) used in GAMINR is a 95-group spectrum obtained from the full core calculation in both the fuel and reflector regions. The photon interaction cross sections are dependent on the elemental composition and incoming photon energy. A comparison of various cross sections between values produced with NJOY and values produced by MCNP are included in Figures 10 and 11 for the fuel and reflector regions, respectively. These plots show that there is good agreement between the codes in both material regions. NJOY tends to under-predict the photoelectric absorption and heating in the lower energy range.

The various MCNP photon cross sections are added to an ISOXML formatted file to be read by Griffin. The photon transfer matrices necessary for the multigroup solvers are

obtained by rescaling the NJOY transfer matrices as to preserve the total scattering cross section from MCNP. Again, here we assume that the shape of the group-to-group transfer cross-section matrix computed in NJOY is accurate until the independent capability is incorporated to Griffin. The scaling factor is computed with

$$S_m = \frac{\sum_{m'=1}^{M} \Sigma_{m\Rightarrow m'}^{ref}}{\sum_{m'=1}^{m} \Sigma_{m\Rightarrow m'}}, \tag{3}$$

where

- $\Sigma_{m\Rightarrow m'}^{ref}$ is the reference-scattering production cross section for neutron group m
- $\Sigma_{m\Rightarrow m'}$ is the NJOY photon-scattering production cross section for neutron group m
- S_m is the scaling factor for group m

3.3 Model Description

The simplified 1-D cylindrical graphite reactor model used in this work contains one active core region and one reflector region. A representation of the model is shown in Figure 12. The dimensions are representative of typical graphite moderated power reactors designs like the HTR-PM [7].

The various cross-section regions and compositions are included in Table 5. Only two isotopes are used in order to simplify the data preparation step.

Table 5: Simplified 1-D cylindrical graphite reactor model

Region	Radius [cm]	number XS regions	number mesh intervals	Composition [at/barn-cm]
Fuel	150.0	6	150	$^{235}U(8.00x10^{-7})$, $^{12}C(8.00x10^{-2})$
Reflector	250.0	4	100	$^{12}C(8.00x10^{-2})$

Figure 13 shows a schematic of the coupling between the Griffin neutron- and photon-transport calculations. There are two inputs: a neutron-transport k-eigenvalue problem and

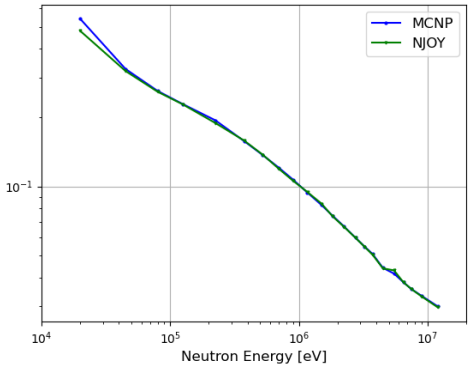

(a) total [cm^{-1}]

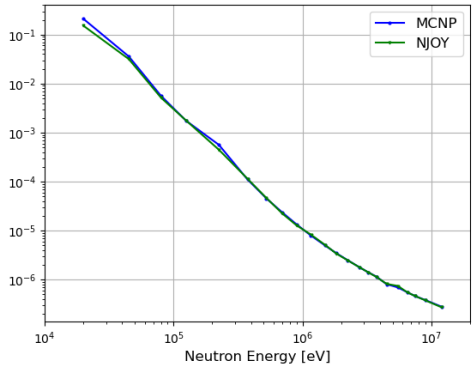

(b) PE absorption [cm^{-1}]

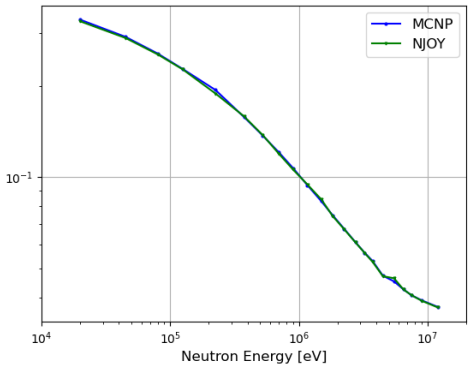

(c) total scattering production [cm^{-1}]

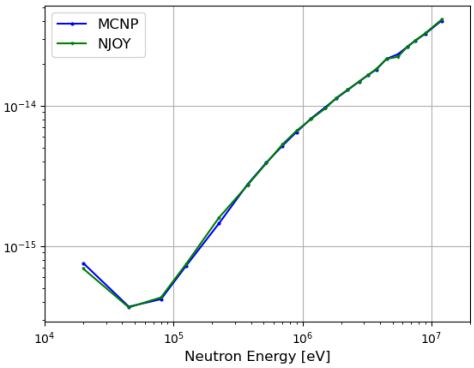

(d) heating [J-cm^{-1}]

Figure 10: Comparison of photon cross sections for the fuel between MCNP 6.1 and NJOY21

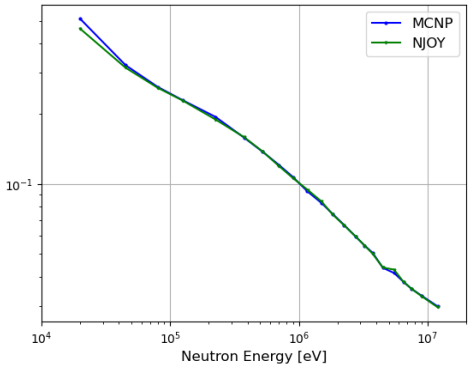

(a) total [cm^{-1}]

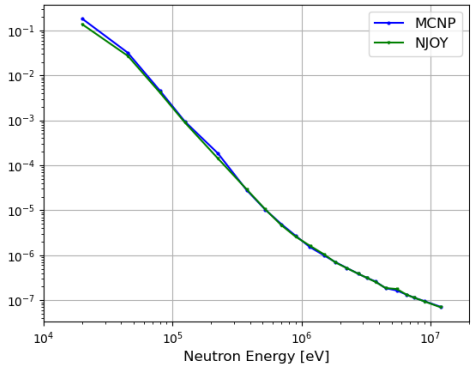

(b) PE absorption [cm^{-1}]

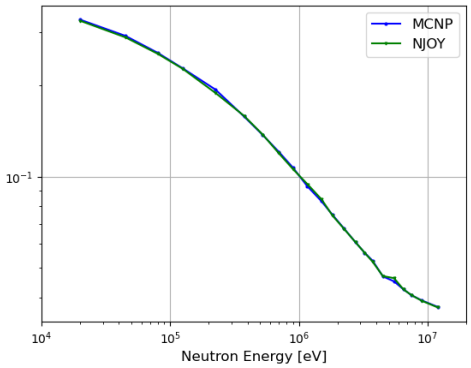

(c) total scattering production [cm^{-1}]

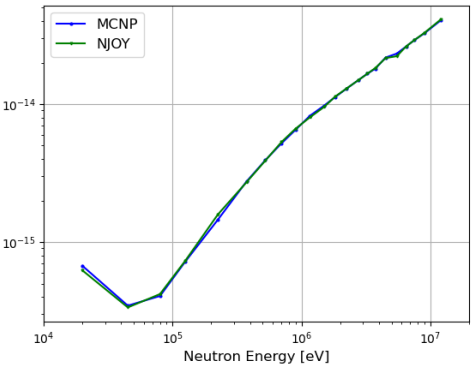

(d) heating [J-cm^{-1}]

Figure 11: Comparison of photon cross sections for the reflector between MCNP 6.1 and NJOY21

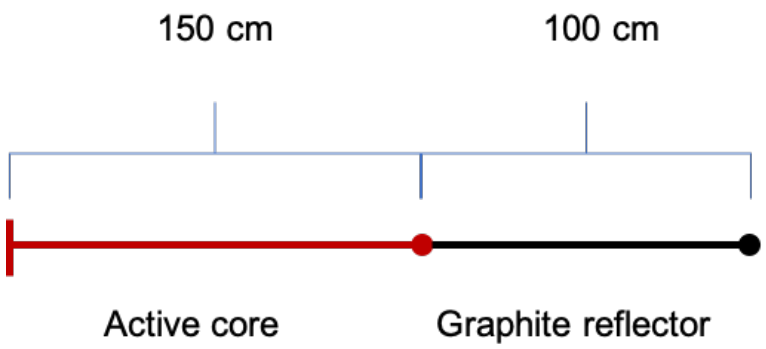

Figure 12: Simplified 1-D cylindrical graphite reactor model

a photon-transport source problem. The photon transport problem is the main application while the neutron transport is the sub application. The neutron transport eigenvalue solution provides the photon source to the photon-transport source problem. The photon source is transferred with the transfer type *CoupledParticleTransfer*. The neutron heating is also transferred to compute the total energy deposition in the core.

For the neutron transport solution, Griffin employs a P3 scheme with linear anisotropic scattering. The photon-transport problem is solved with a P5 scheme with matching scattering Legendre order.

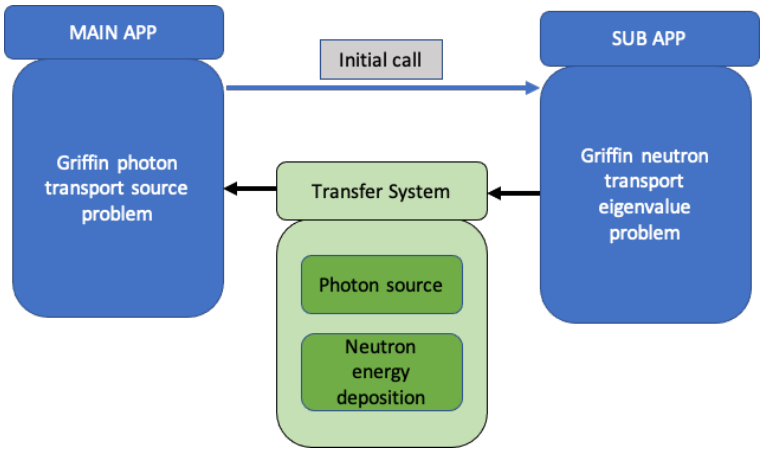

Figure 13: Coupled neutron-photon calculation in Griffin

3.4 Results

The fundamental mode eigenvalue results are included in Table 6. Both CE MC codes are within the uncertainty of the calculation, whereas the Griffin multigroup is 240 pcm higher, which is not unexpected since no homogenization equivalence is in use. The photon production rate compares well between the various codes.

Table 6: Fundamental mode eigenvalues and total photon source

Code	keff	rel. uncert. / error [pcm]	total photon source [photons/lost particle]
MCNP	1.06494	2	4.5764
Serpent	1.06490	2	4.5762
Griffin	1.06747	257	4.5759

The neutron heating results are shown in Figure 14. There is excellent agreement between the two Monte Carlo codes, for the exception to the farthest reflector region, where there is a disagreement of roughly 1%. The Griffin neutron heat deposition solution is within 0.2% of the MC reference in the active core region. The solution is also within 1% in the first reflector cross-section zone, but quickly degrades. This large difference in the reflector zone is due to differences in the fast flux solution, which dominates the energy deposition in the reflector. This deficiency can be improved with a combination of better cross sections and higher order neutron transport, but it is seldom used due to the small contribution from neutron heating in non-fueled regions.

The gamma heating component is depicted in Figure 15. The MC codes are in reasonable agreement with a maximum difference near 1% in the reflector zone. The Griffin solution overpredicts the photon energy deposition in the active core region by roughly 2.4% and again degrades in the reflector region to a maximum value of 1.5%.

The distribution of the total heating is shown in Figure 16. The neutron heating dominates the energy deposition in the active core region whereas the photon heating dominates the reflector region. Table 7 includes the energy deposition contribution by particle type in the different regions of the core for the three codes used in this work.

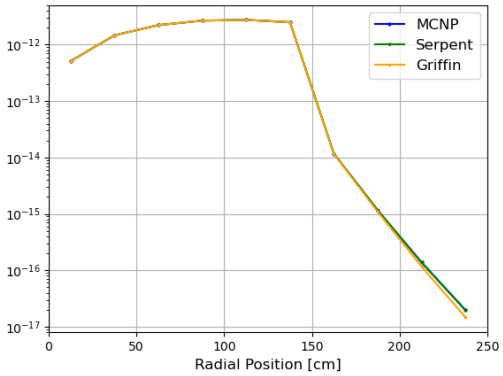

(a) neutron heating

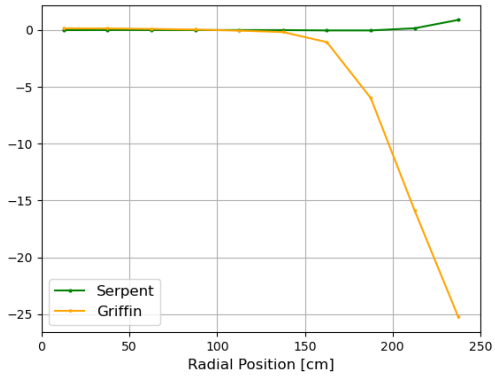

(b) % difference in neutron heating

Figure 14: Comparison of neutron heating values against the MCNP reference

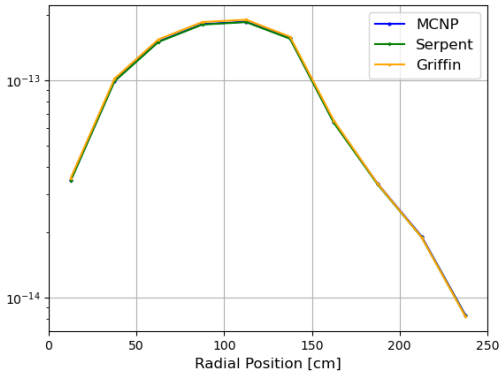

(a) % photon heating

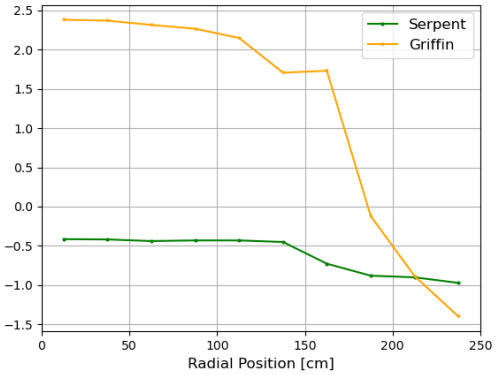

(b) % difference in photon heating

Figure 15: Comparison of photon heating values against the MCNP reference

Table 7: Allocation of the energy deposition per particle type in the active and reflector zones

Code	MCNP	Serpent	Griffin
neutron heating – active core	92.803%	92.835%	92.676%
neutron heating – reflector	0.099%	0.099%	0.097%
photon heating – active core	6.146%	6.121%	6.270%
photon heating – reflector	0.953%	0.945%	0.957%

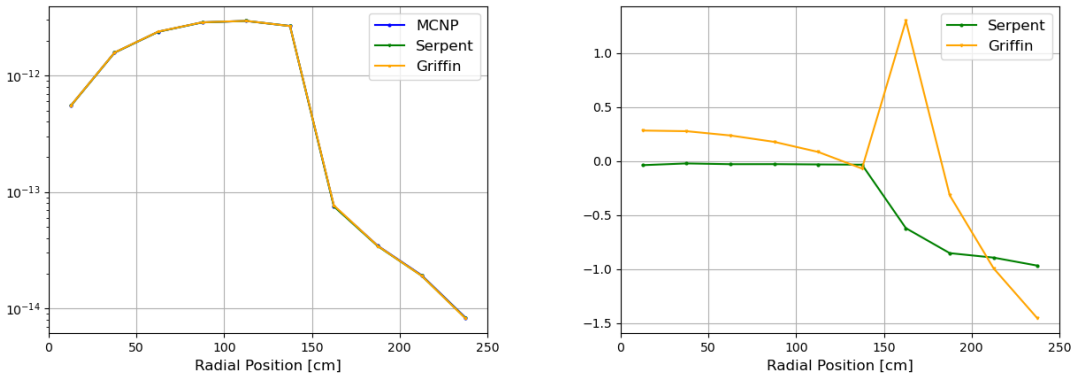

(a) total heating

(b) % difference in total heating

Figure 16: Comparison of the total heating values against the MCNP reference

4 CONCLUSIONS

This report details progress and activities of Idaho National Laboratory (INL) on the Nuclear Regulatory Commission (NRC) project "Development and Modeling Support for Advanced Non-Light Water Reactors." We report the successful completion of one task of the NRC project "Development and Modeling Support for Advanced Non-Light Water Reactors." In addition, the extended scope tasks have also been completed. The following task completions are reported:

- Task 3a: A prototypical 2-D microreactor model with control drums in the reflector was modeled in Griffin and Serpent. Serpent was used to generate reference results as well as cross sections for use in Griffin. The Griffin model used cross section and SPH factor libraries of varying fidelity to study Griffin's cross section interpolation, SPH factor interpolation, and rod-cusping treatment. Overall, Griffin was able to successfully model control drum rotation. Conclusions are not drawn regarding the specific number of discrete drum rotations necessary to build a library capable of capturing eigenvalue and reactions rates to a pre-specified accuracy since it is expected that this will be problem dependent.
- Task 3c: A simplified 1-D graphite reactor model with non-local neutron and photon heating was developed and tested with MCNP, Serpent, and Griffin. The multigroup data preparation for thermal neutron systems is not currently implemented in the Griffin application, but it is slated for FY-21. Instead, Serpent and NJOY were used to prepare the neutron cross sections and photon production matrix, whereas MCNP and NJOY were used to prepare the gamma library. The current data is not ideal for this calculation but it leads to reasonable agreement between the various solutions. The Griffin code used a third-order spherical harmonics approximation with P1 scattering for the neutron transport solution and fifth-order photon transport solution with matching scattering order. The Griffin coupling relies on the MOOSE MultiApp system to perform the eigenvalue calculation (SubApp) and then transfer the gamma source to the photon source problem (MainApp). The Griffin neutron energy deposition is the active core region is within 0.3% of the reference, but it degrades in the reflector regions to -1.5%. The photon energy deposition is overpredicted in the active core by 2.4% and underpredicted in the reflector zone with a maximum difference of -1.5%. The simulation shows that the coupled neutron-gamma calculation is now achievable with Griffin. Overall, the results look promising and future analysis should use an improved data stream and focus on determining the potential cancellation of error within each energy group.

References

[1] J. Ortensi et al. "A Newton solution for the Superhomogenization method: The PJFNK-SPH". In: *Annals of Nuclear Energy* 111 (Jan. 2018), pp. 579–594.

[2] Sebastian Schunert et al. "Control rod treatment for FEM based radiation transport methods". In: *Annals of Nuclear Energy* 127 (2019), pp. 293–302. ISSN: 0306-4549. DOI: https://doi.org/10.1016/j.anucene.2018.11.054. URL: http://www.sciencedirect.com/science/article/pii/S0306454918306534.

[3] G. Hua et al. *Multi-Physics Simulations of Heat Pipe Micro Reactor*. ANL report ANL/NSE-19/25. Argonne National Laboratory, 2019.

[4] T. Goorley et al. "Initial MCNP6 Release Overview". In: *Nuclear Technology* 180 (Dec. 2012), pp. 298–315.

[5] J. Leppänen. "Development of a New Monte Carlo Reactor Physics Code". PhD thesis. Helsinki University of Technology, 2007.

[6] R.E. MacFarlane and A.C. Kahler. "Methods for Processing ENDF/B-VII with NJOY". In: *Nuclear Data Sheets* 111.12 (2010). Nuclear Reaction Data, pp. 2739–2890. ISSN: 0090-3752. DOI: https://doi.org/10.1016/j.nds.2010.11.001. URL: http://www.sciencedirect.com/science/article/pii/S0090375210001006.

[7] Jingyu Zhang, Fu Li, and Yuliang Sun. "Physical Analysis of the Initial Core and Running-In Phase for Pebble-Bed Reactor HTR-PM". In: *Science and Technology of Nuclear Installations* 8918424 (2017).